

Fuzzy Symbolic Dynamics for Neurodynamical Systems

Krzysztof Dobosz¹ and Włodzisław Duch²

¹ Faculty of Mathematics and Computer Science,
Nicolaus Copernicus University, Toruń, Poland

kdobosz@mat.umk.pl

² Department of Informatics, Nicolaus Copernicus University, Toruń, Poland
Google: W. Duch

Abstract. Neurodynamical systems are characterized by a large number of signal streams, measuring activity of individual neurons, local field potentials, aggregated electrical (EEG) or magnetic potentials (MEG), oxygen use (fMRI) or concentration of radioactive traces (PET) in different parts of the brain. Various basis set decomposition techniques that try to discover components that carry meaningful information are used to analyze such signals, but these techniques tell us little what the whole system is doing. Fuzzy Symbolic Dynamics (FSD) may be used for dimensionality reduction of high-dimensional signals, defining non-linear mapping that may be used for visualization of the trajectories that define the state of the whole system. Global visualization of high-dimensional trajectories shows various aspects of signals that are difficult to discover looking at individual components, or to notice observing dynamical visualizations. FSD can be applied to raw signals, transformed signals (for example, ICA components), or to signals defined in the time-frequency domain. Visualization of a model system with artificial radial oscillatory sources, and of the output layer (50 neurons) of a neural Respiratory Rhythm Generator model (RRG) that includes 300 spiking neural units, are presented to illustrate the method.

1 Introduction

Neurodynamical systems are characterized by multiple streams of nonstationary data, and thus may be represented only in highly dimensional signal spaces. Electrical activity of neurons is observed in multielectrode recordings, local field potentials or electrocorticographic or electroencephalographic recordings with up to 256 electrodes and sampling frequency of one millisecond. A large number of neuroimaging methods produce even more streams of data. Understanding of such signals is not easy because of high volume of data that quickly changes in time. Simulation of complex dynamics is usually described in terms of basins of attractors, but precise characterization of these basins, relations between them in terms of possible transitions, is never attempted.

Popular signal processing techniques include removal of artifacts by various filtering techniques, waveform analysis, morphological analysis, decomposition of data streams into meaningful components using Fourier or Wavelet Transforms, Principal Component Analysis (PCA), Independent Component Analysis (ICA), etc [1, 2]. Interesting events are then searched for using processed signal components, with time-frequency-intensity colored maps showing how the processes unfold. Such techniques

are very useful, but do not show global properties of the processes in the high-dimensional signal spaces. Global analysis is needed to see attractors that trap dynamics, characterize the type of system's behavior, notice partial desynchronization or high frequency noise that blurs the trajectories. For brain-computer interfaces and other applications a static snapshot of the whole trajectory, showing its main characteristics, could be very useful.

In this paper a radically different approach to high-dimensional signal analysis is investigated (to focus attention we shall talk about neurodynamics, although any dynamical system can be analyzed in this way). Most important properties of the dynamics may be uncovered if dimensionality of the problem is sufficiently reduced. This is done with the help of fuzzy symbolic dynamics (FSD). To see the trajectories of the global system state "probes", or localized functions that are activated in a different way by the trajectories that pass near their center, are placed in the signal space. Using k such functions, strategically placed in important points of the signal space, a non-linear reduction of dimensionality suitable for visualization of trajectories is achieved. Inevitably a lot of details will be lost but with a proper choice of parameters the information that correlates with observed behavior or experimental task may be preserved, while irrelevant information will be suppressed.

In the next section FSD mapping that captures interesting properties of trajectories is described. To understand how to set up mapping parameters and how to interpret resulting images a model EEG situation is analyzed in Sec. 3, with several sources of radial waves placed in a mesh, and sensors that record the amplitude of the incoming waves in different points of the mesh. As an example of real application in Sec. 4 trajectory visualizations for neural Respiratory Rhythm Generator model (RRG) are analyzed. The final section contains a brief discussion with a list of several open questions.

2 Fuzzy Symbolic Dynamics

Assume that some unknown sources create a multi-dimensional signal that is changing in time, for example an EEG signal measured by n electrodes:

$$x(t) = \{x_i(t)\} \quad i = 1, \dots, n \quad t = 0, 1, 2, \dots \quad (1)$$

Vectors $x(t)$ represent the state of the dynamical system at time t , forming a trajectory in the signal space. Observing the system for a longer time should reveal the landscape created by this trajectory, areas of the signal space where the state of the system is found with the highest probability, and other areas where it never wanders. Recurrence maps and other techniques may be used to view this trajectory, but do not capture many important properties that it reflects.

In the symbolic dynamics [3] the signal space is partitioned into regions that are labeled with different symbols, emitted every time the trajectory is found in one of the regions. The sequence of symbols gives a coarse-grained description of dynamics that can be analyzed using statistical tools. Dale and Spivey [4] argue that symbolic dynamics gives an appropriate framework for cognitive representations, although discretization of continuous dynamical states loses the fluid nature of cognition. Symbols obviously

reduce the complexity of dynamical description but partitioning of highly-dimensional signal spaces into regions with sharply defined boundaries is highly artificial.

The notion of symbolic dynamic is generalized here in a natural way to a Fuzzy Symbolic Dynamics (FSD). Instead of discrete partitioning of the signal space leading to symbols, interesting regions are determined analyzing probability density $p(x)$ of finding the trajectory $x(t)$ in some point x , averaging over time. Local maxima of this probability define quasi-stable states around which trajectories tend to clusters. Such maxima may serve as centers μ_k of prototypes associated with fuzzy membership functions $y_k(x; \mu_k)$ that measure the degree to which the $x(t)$ state belongs to the prototype μ_k . Membership functions may be defined using knowledge-based clustering [5], or as prototype-based rules with context-based clustering techniques [6]. Context is defined by questions that are of interest, for example discrimination between different experimental conditions, or searching for invariants in one of these conditions. For visualization two Gaussian membership functions are quite useful:

$$y_k(x; \mu_k, \Sigma_k) = \exp\left(- (x - \mu_k)^T \Sigma_k^{-1} (x - \mu_k)\right) \quad (2)$$

In some cases diagonal dispersions Σ_k are sufficient, suppressing irrelevant signals, but general covariance matrices (used in Mahalanobis distance) may extract more meaningful combinations of signals that correlate with experimental conditions, or with qualities that may be estimated in a subjective way. Such brain-mind mapping will be closer to the idea of cognitive representations than symbolic dynamics [4]. Symbolic description may be easily generated by strongly activated prototypes, but other prototypes may correspond to sensorimotor actions that are not directly connected with symbolic labels.

Selecting only two prototypes trajectories $x(t)$ may be visualized in a two-dimensional space $\{y_i(t), y_j(t)\}$. If all Gaussian components have the same variance a single parameter will define dispersion. For visualization each pair of functions should have sufficiently large dispersions σ_i and σ_j to cover the space between them, for example:

$$\sigma_i = \sigma_j = \frac{1}{2} \|\mu_i - \mu_j\| \quad . \quad (3)$$

3D visualization can also be done by plotting transformed points for three clusters, one for each dimension. Dispersions should then be set to the largest among the 3 pairs. Pairwise plots can be used to observe trajectory from different points of view. Normalization of vectors in the signal space is assumed. If the goal is to distinguish several experimental conditions optimization of parameters of membership functions can be done using learning techniques to create clear differences in corresponding maps. Adding more localized functions in some area where dynamics is complex will show fine structure of the trajectory.

An alternative to fuzzy membership functions is to define reference points in the signal space, and measure the distance between the trajectory and these points using some metric function. Non-linear metric functions should have some advantage in analysis of neurodynamics, as the influence of the trajectory on prototypes should sharply decrease to zero with the distance, reflecting non-linear properties of neurons. We shall not consider here adaptation of parameters or distance-based visualization, concentrating instead on the interpretation of global mappings. To understand the process better a mixture of artificial radial and linear wave sources is analyzed in the next section.

3 Plane and radial waves on a grid

To understand the structure of complex EEG and similar signals a very simple artificial model has been created. Sensors are placed on a quadratic grid with $n \times n$ points, where plane and radial waves generated by several sources are traveling, creating additive patterns and activating these sensors. Similar assumptions are made about electric potentials reflecting neuronal activity in the brain (for example, in the low resolution electromagnetic tomography, LORETA³).

The grid has equally spaced points $p_{ij} = (x_i, y_j)$ inside the square:

$$x_i, y_j \in \left\{ 0, \frac{1}{n-1}, \dots, \frac{n-2}{n-1}, 1 \right\} \quad i, j = 1, \dots, n . \quad (4)$$

The activation of the sensor due to a plane wave $F^{(l)}(t, x)$ traveling through the square in the grid point p_{ij} at the time $t = 0, 1, 2, \dots$ is given by the equation:

$$F^{(l)}(t, p_{ij}) = \cos(\omega_l t - \mathbf{k}_l \cdot \mathbf{p}_{ij}) , \quad (5)$$

where ω_l is the frequency of the wave (defining time intervals), the wave vector \mathbf{k}_l defines the direction of the wave movement and its length is equal to the inverse of the wave length and \mathbf{p}_{ij} is the vector pointing to the grid point p_{ij} . Thus, for horizontal plane wave ($\mathbf{k} = \|\mathbf{k}\| [1, 0]^T$) formula (5) becomes:

$$F(t, p_{ij}) = \cos(\omega t - k x_i) . \quad (6)$$

Radial wave reaching the sensor at grid point p_{ij} leads to an activation:

$$R^{(l)}(t, p_{ij}) = \cos(\omega_l t - k_l r^{(l)}) , \quad (7)$$

where

$$r^{(l)} = \sqrt{(x_i - x_0^{(l)})^2 + (y_j - y_0^{(l)})^2} \quad (8)$$

is the distance between point p_{ij} and the wave source (x_0, y_0) .

The final activation $A(t, p_{ij})$ of the sensor in point p_{ij} at time $t = 0, 1, 2, \dots$ is obtained by summing and normalizing all wave values in every grid point:

$$A(t, p_{ij}) = \left(\sum_{l=1}^{N_f} F^{(l)}(t, p_{ij}) + \sum_{l=1}^{N_r} R^{(l)}(t, p_{ij}) \right) / (N_f + N_r) . \quad (9)$$

Sensor activations form a $n \times n$ matrix $A(t)$ containing values for all sensors at time t . Elements of $A(t)$ are defined in n^2 -dimensional signal space and are in the $[-1, 1]$ interval. Gaussian membership functions (2) may serve as probes (detectors of activity) in this space. Placing their centers in two opposite vertices of the hypercube $S = [-1, 1]^{n^2}$:

$$\mu_1 = [-1, \dots, -1]^T \quad \mu_2 = [1, \dots, 1]^T \quad (10)$$

³ See <http://www.unizh.ch/keyinst/loreta>.

the membership functions take all n^2 sensor activations $A(t)$ as their argument:

$$G_k(A(t); \mu_k, \sigma_k) = \exp\left(-\frac{\|A(t) - \mu_k\|}{2\sigma_k^2}\right), \quad (11)$$

where σ_k is the dispersion.

A lot of experiments have been conducted using the 16×16 grid with 256 points (maximum number of electrodes used in real EEG experiments), and various number of stationary and non-stationary sources, frequencies and directions. For this grid $\sigma_1 = \sigma_2 = \|\mu_1 - \mu_2\|/10$ gives relatively wide range of sensor activations. In Fig. 1 examples of trajectories for one and two radial waves are presented, using $\omega = 0.1$, which is sufficient for smooth trajectory change, and the wave vector length $\|k\| = 2\pi$.

Specific position of sources and combinations of planar and radial waves may be identified with correct placement of centers and dispersions of the membership functions.

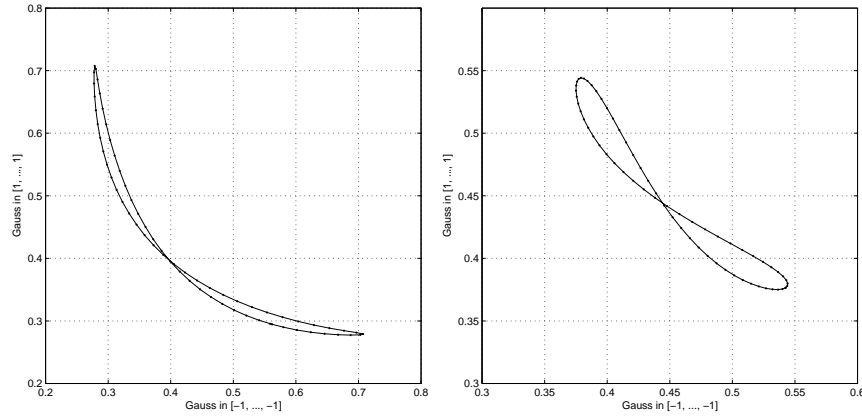


Fig. 1. Trajectories for one radial wave with the source at point $(\frac{1}{2}, \frac{1}{2})$ (left side), and two radial waves with the sources at $(\frac{1}{4}, \frac{1}{4})$ and $(\frac{3}{4}, \frac{3}{4})$ (right side).

4 Visualization of the activity of Respiratory Rhythm Generator

FSD approach has been used to study behavior of the neural Respiratory Rhythm Generator model (RRG). The RRG is a parametric neural network model constructed from three populations of spiking neurons: beaters (200 in the model), bursters (50 units) and followers (50 units). The last population produce an output of model activity that is used for synaptic excitation of motoneurons and in consequence control of upper and lower lung muscles. Our implementation of RRG is based on the spiking neural network model described in [7, 8].

Below visualization of the followers (output layer neurons) is examined. The first trajectory for time series corresponding to a single burst is presented in Fig. 2. The number of samples along these trajectory was 49090, each vector containing membrane potentials of 50 follower cells (normalized in every dimension). Clusterization was done with the k -means algorithm, for two clusters where Gaussian probe functions have been placed. Trajectories have been drawn with a thick pen to account for a jitter that blurs them when longer time sequences are taken.

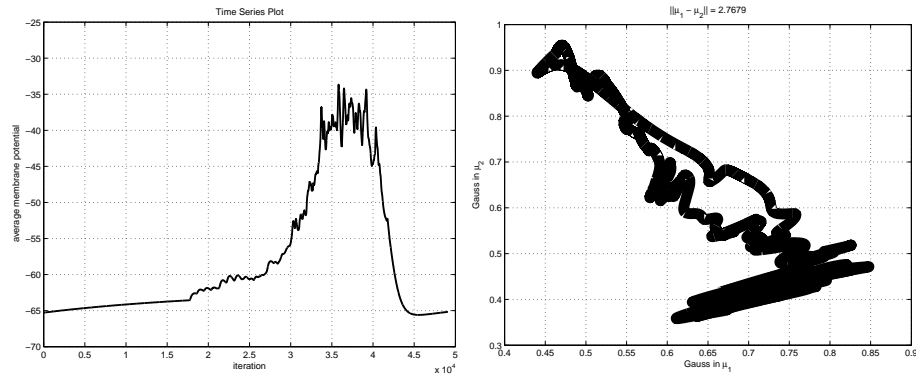


Fig. 2. The time series plot (left) representing average membrane potential (sum of all potentials divided by the number of neurons) versus iteration number, and the mapping of the corresponding trajectory (right).

Figure 3 shows trajectory for the same time series as the Fig. 2, zooming on one of the attractors to show details of oscillation around it. This attractor corresponds to oscillations visible in the highest part of the time series plot (Fig. 2 left). Generating more bursts slowly fill the whole area with trajectories giving almost uniform probability of finding the system there. This shows chaotic behavior of the system at the peak of activity.

A common visualization technique in analysis of neural dynamics is to show plots of activations for selected pairs of neurons. In Fig. 4 two different pairs are shown. Unfortunately with 50 neurons there are 1225 possible pairs and most of them show quite different plots, although the global dynamics is much more stable. Thus pairwise visualization of single neuron activity does not provide much useful information.

In Fig. 5 three cluster centers have been defined using the k -means algorithm ($k = 3$). Pairwise diagrams show trajectories for all three cluster pairs. Distances between cluster centers are printed above the graphs. The second pair is more sensitive to variability that appears during building of the discharge activity, showing quite a bit of variance in this process.

The RRG model may generate various rhythms that correspond to different breathing patterns. Trajectory examples in Fig. 6 compare two distinct cases, one for normal, regular burst generation, and one for pathological case with different burst strengths

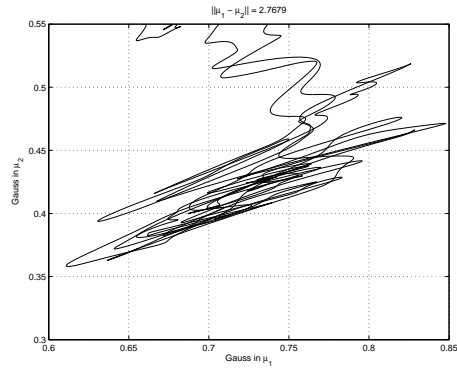


Fig. 3. Zoomed area of trajectory for time series with one burst around main attractor.

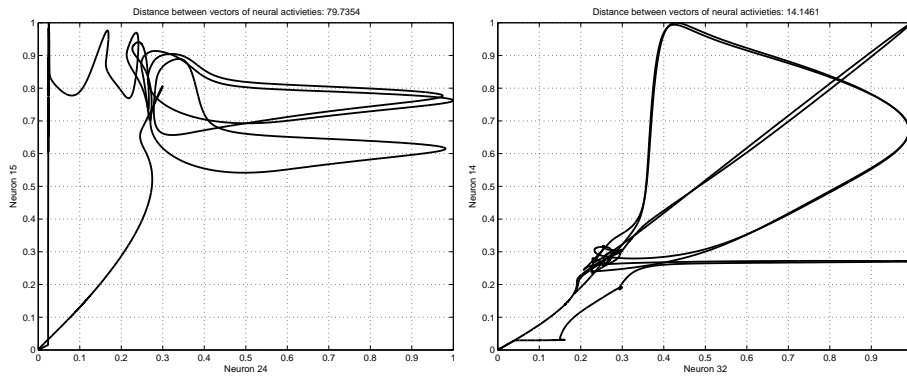


Fig. 4. Neural activity plots for 2 neurons from RRG that have the most (left) and the least (right) different vectors of neural activities.

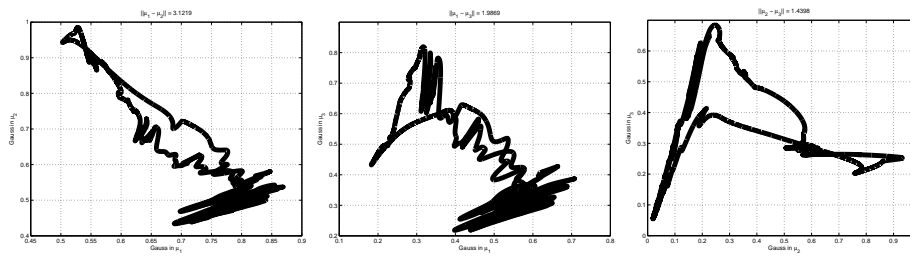


Fig. 5. Pairwise diagrams for 3 clusters found by k-means algorithm representing trajectories for time series with one burst.

(i.e. different peak heights). The trajectories have been drawn using 19600 vectors, each containing values of membrane potentials of 50 follower cells, covering about 20 spikes. Two clusters have been found using the k -means algorithm, and the same parameters of membership functions used in both cases. Pathological case seems to reach the same amplitude but as a whole behaves quite differently, reaching much smaller values in first dimension, due to the lack of synchronization between different output neurons.

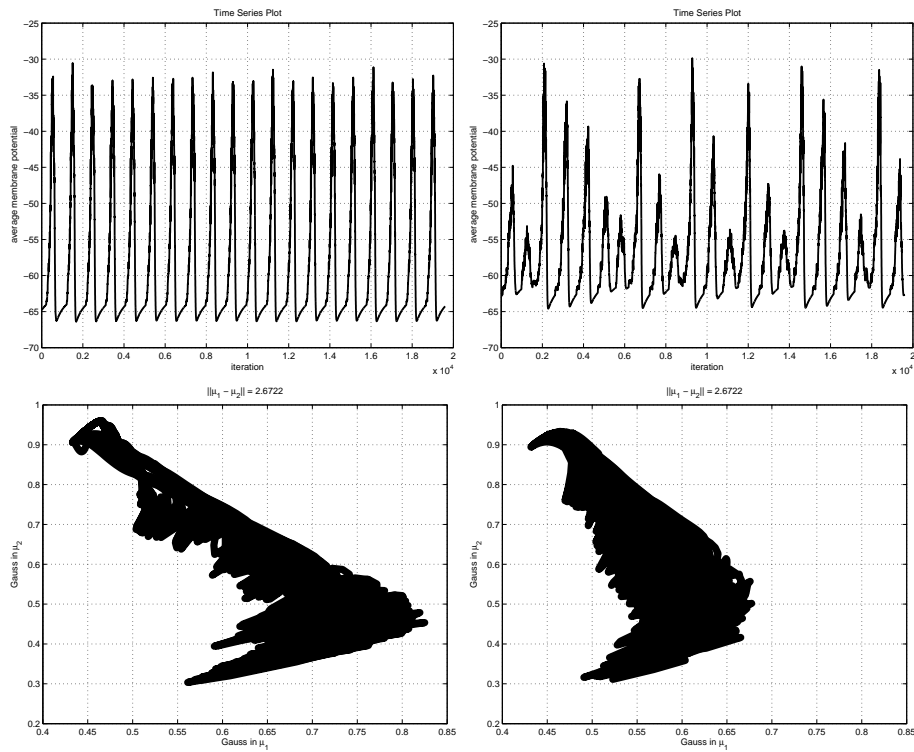


Fig. 6. Trajectory plots (bottom) done with thick pen for 19600 vectors containing membrane potentials of 50 follower cells from RRG, and time series plots (top) representing average membrane potential vs. iteration number. Graphs on the left correspond to a normal rhythm case, and on the right to a pathological one, both presented using the same membership functions.

When two similar time series plots are compared small differences between them may not be noticeable. The FSD method is sensitive to small changes in the global dynamical state and consequently it allows for quite accurate comparison. Figure 7 compares two normal rhythms that differ only slightly. Time series plots look very similar but global trajectories in FSD graphs show significant differences.

In all examples presented in this section dispersions of Gaussians were set to the half of the distance between centers ($\|\mu_1 - \mu_2\| / 2$) to cover the signals that are between the centers.

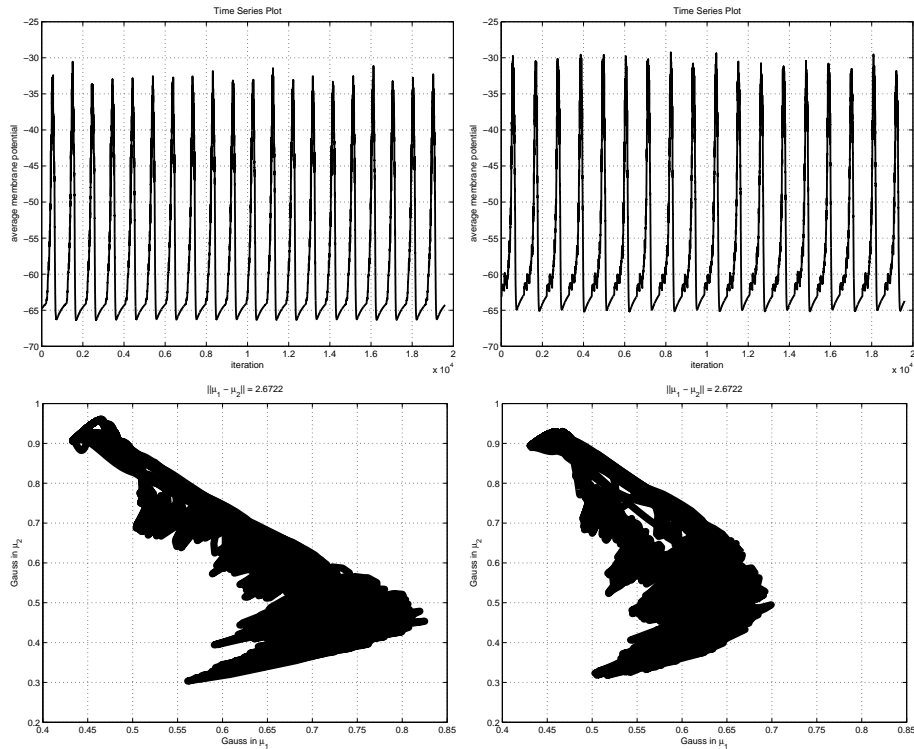


Fig. 7. Comparison of two similar normal rhythm cases. Time series plots (top) looks very similar while trajectory plots (bottom) differ noticeable. In both cases sample of 19600 vectors have been used.

5 Discussion

Symbolic dynamics has found many applications, while its fuzzy version has never been developed. It seems to be a very interesting method that should find many applications. In this paper it has been applied to visualization of high-dimensional neurodynamical systems. Many aspects of dynamics may be analyzed using this technique:

1. In which part of the signal space the state of the system spends most of its time?
2. How many attractors can be identified?
3. What are the properties of different basins of attractors (large and shallow, or narrow and deep)?

4. What are the probabilities of transition between them?
5. What type of oscillations occur around the attractors?

Quantitative measures to compare different dynamical systems should be introduced, for example:

- the number of attractors;
- percentage of time spent by the system in a given attractor basin;
- character of oscillations around attractors, including some measures of chaos;
- distances between attractors, measured by the time of transitions;
- probabilities of system transitions between attractors.

Such measures will give interesting characterization of dynamical systems. Application of FSD to recurrent networks should show transitions between their states. Applications to real EEG signals will require careful optimization of membership functions, with conditional clustering to remove irrelevant information by finding most informative center locations and weights for different signals. Visualization of highly-dimensional trajectories obviously depends on what aspects of the system behavior are of interest. Methods of parameter adaptation that include context [5, 6] will soon be applied to visualization of real experimental data. For strongly non-stationary signals the whole landscape containing basins of attractors may slowly rotate, preserving relations between main attractors. For example, change in the level of neuromodulation may influence the landscape by increasing the overall activations in some regions of signal space. Parametrization of probes that should then change in time to counter this effect would be important. The great challenge is to find meaningful combinations of signals that are correlated with inner experiences, or find quantitative measures of the FSD low dimensional representations that would be useful in brain computer interfaces.

References

1. Rangayyan, R.M.: Biomedical Signal Analysis: A Case-Study Approach. IEEE Press Series on Biomedical Engineering. Wiley-IEEE Press (2001)
2. Sanei, S., Chambers, J.A.: EEG Signal Processing. Wiley (2008)
3. Lin Hao, B., Zheng, W.M., eds.: Applied Symbolic Dynamics and Chaos. World Scientific (1998)
4. Dale, R., Spivey, M.J.: From apples and oranges to symbolic dynamics: a framework for conciliating notions of cognitive representation. *Journal of Experimental & Theoretical Artificial Intelligence* **17**(4) (2005) 317–342
5. Pedrycz, W.: Knowledge-Based Clustering: From Data to Information Granules. Wiley-Interscience (2005)
6. Blachnik, M., Duch, W., Wierzchowski, T.: Selection of prototypes rules – context searching via clustering. *Lecture Notes in Artificial Intelligence* **4029** (2006) 573–582
7. Butera, R., Rinzler, J., Smith, J.: Models of respiratory rhythm generation in the pre-bötzinger complex: I. bursting pacemaker neurons. *Journal of Neurophysiology* **82** (1999) 382–397
8. Butera, R., Rinzler, J., Smith, J.: Models of respiratory rhythm generation in the pre-bötzinger complex: II. populations of coupled pacemakers. *Journal of Neurophysiology* **82** (1999) 398–415